Inorganic Chemistry
Article

Inorg. Chem. **2009**, *48*, 8559–8568 **8559**
DOI: 10.1021/ic802128r

Reactivity of Neutral $Mo(S_2C_6H_4)_3$ in Aqueous Media: an Alternative Functional Model of Sulfite Oxidase.

Francisco Pérez Pla,* Antonio Cervilla, María Piles, and Elisa Llopis

Instituto de Ciencia de Materiales de la Universidad de Valencia (ICMUV), P.O. Box 2085, Poligono La Coma, Paterna, Valencia, Spain

Received November 6, 2008

The kinetics of the reaction of neutral $[Mo(S_2C_6H_4)_3]$ with hydrogen sulfite to produce the anionic Mo(V) complex, $[Mo(S_2C_6H_4)_3]^-$, and sulfate have been investigated. It has been shown that $[Mo(S_2C_6H_4)_3]$ acts as the electron−proton sink in the oxygenation reaction of HSO_3^- by water. Reaction rates, monitored by UV/vis stopped-flow spectrometry, were studied in THF/water media as a function of the concentration of HSO_3^- and molybdenum complex, pH, ionic strength, and temperature. The reaction exhibits pH-dependent HSO_3^- saturation kinetics, and it is first-order in complex concentration. The kinetic data and MS-ESI spectra are consistent with the formation of $[Mo\,O(S_2C_6H_4)_2(S_2C_6H_5)]^-$ (**1**) adduct as a crucial intermediate that transfers the oxygen atom to HSO_3^- yielding the Mo(V) species quantitatively.

Introduction

Molybdoenzymes are known to catalyze oxidation−reduction reactions that are essential in the metabolism of carbon, nitrogen, and sulfur. Among them, sulfite oxidase enzymes are oxo-transferases responsible for the physiologically vital oxidation of sulfite to sulfate.[1,2] As one of the most intensively studied molybdoenzymes, sulfite oxidase is generally considered as the prototypical member of a family of molybdoenzymes possessing dioxomolybdenum sites in the fully oxidized Mo(VI) form.[3,4] Transfer of the oxygen atom to substrate (HSO_3^-) and its replacement from water appears to occur in the Mo(VI) to Mo(IV) transformation.[5]

In interpreting oxygen atom transfer (OAT) reaction pathways, two mechanisms are proposed (eqs 1 and 2),[6]

$$Mo^{VI}O_2 + X \rightleftarrows Mo^{VI}O(XO) \rightarrow Mo^{IV}O + XO \quad (1)$$

$$Mo^{VI}O_2 + X \rightarrow Mo^{IV}O + XO \quad (2)$$

In the former, a pre-equilibrium substrate (X) binding reaction is followed by OAT step in a rate-determining first-order reaction at sufficient high X concentration. In the latter, the reaction is first-order in both reactants, and no pre-equilibrium binding influences the kinetics.[7−11] Although reactions of general type 2 are far more common, one example of type 1 has been found with a bis(dithiolene) $Mo^{VI}O_2/Mo^{VI}O$ couple,[12] which provides the cleanest demonstration of the molybdenum mediated oxidation of hydrogen sulfite. The complex $[Mo^{VI}O_2\,(mnt)_2]^{2-}$ (mnt = 1, 2-dicyano-ethylene-dithiolene) performs oxidation of HSO_3^- to SO_4^{2-} similar to the reductive half reaction of native sulfite oxidase in terms of saturation and anionic inhibition inetics. In acetonitrile containing a small amount of water, the reaction monitored spectrophotometrically is following Michaelis−Menten kinetics with $K_M = (k_2 + k_{-1})/k_{+1} = 0.010$ M and $k_2 = 0.87\ s^{-1}$ for the rate-determining step ($1/k_{obs} = 1/k_2 + K_M/k_2[HSO_3^-]$, see eq 3,

$$[Mo^{VI}O_2(mnt)_2]^{2-} + HSO_3^- \underset{k_{-1}}{\overset{k_{+1}}{\rightleftharpoons}} [MO^{VI}O_2(mnt)_2(HSO_3)]^{3-}$$

$$[Mo^{VI}O_2(mnt)_2(HSO_3)]^{3-} \xrightarrow{k_2} [Mo^{IV}O(mnt)_2]^{2-} + HSO_4^- \quad (3)$$

We have recently reported that the $[Mo(S_2C_6H_4)_3]$ complex is capable of catalyzing a rapid OAT reaction from water to

*To whom correspondence should be addressed. E-mail: francisco.perez@uv.es.

(1) Feng, C.; Tollin, G.; Enemark, J. *Biochim. Biophys. Acta* **2007**, 527–539.
(2) Cohen, H.; Betcher-Lauge, S.; Kessler, D.; Rajagopalan, K. *J. Biol. Chem.* **1972**, *247*, 7759–7766.
(3) George, G.; Pickering, I.; Kisker, C. *Inorg. Chem.* **1999**, *38*, 2539–2540.
(4) Kisker, C.; Schindelin, H.; Pacheco, A.; Wehbi, W.; Garret, R.; Rajagopalan, K.; Enemark, J.; Rees, D. *Cell* **1997**, *91*, 973.
(5) Hille, R. *J. Biol. Inorg. Chem.* **1997**, *2*, 804–809.
(6) Enemark, J.; Cooney, J.; Wang, J.; Holm, R. *Chem. Rev.* **2004**, *104*, 1175.
(7) Wang, J.; Tessier, C.; Holm, R. *Inorg. Chem.* **2006**, *45*, 2979–2988.
(8) Jiang, J.; Holm, R. *Inorg. Chem.* **2005**, *44*, 1068–1062.
(9) Sung, K.; Holm, R. *Inorg. Chem.* **2001**, *40*, 4518–4525.
(10) Sung, K.; Holm, R. *J. Am. Chem. Soc.* **2002**, *124*, 4312–4320.
(11) Sung, K.; Holm, R. *J. Am. Chem. Soc.* **2001**, *123*, 1931–1943.
(12) Das, S.; Chaudhury, P.; Biswas, D.; Sarkar, S. *J. Am. Chem. Soc.* **1994**, *116*, 9061–9070.

Published on Web 07/30/2009

tertiary organic phosphines.[13] These systems also display phosphine saturation kinetics. With results from phosphine reactions at hand, we have turned our attention to other physiologically relevant reducing agents such as hydrogen sulfite. The main conclusion arising from this study is that direct reaction of hydrogen sulfite with [Mo($S_2C_6H_4$)$_3$] in THF/H_2O media produces sulfate, which is the key reaction of sulfite oxidase, and causes a fast reduction to the Mo(V) monoanion following a mechanism similar to that previously outlined for organic phosphines. Therefore, [Mo($S_2C_6H_4$)$_3$] can be considered as a functional analogue[6,14] of the active sulfite oxidase site, which coordinates a water molecule and transfers the oxygen atom to the substrate sulfite.

Experimental Section

Materials. The preparation and purification of neutral tris(benzene-1,2-dithiolate) molybdenum, [Mo($S_2C_6H_4$)$_3$], has been previously reported.[15] Only recrystallized samples were used for kinetics measurements. Unless otherwise indicated, all reactions were conducted under Ar. Anhydrous tetrahydrofuran (THF) was distilled from CaH_2, while water of low conductivity was bidistilled prior to use. Both solvents were degassed and infused with Ar. Only fresh distilled solvents were used to prepare solutions. Hydrogen sulfite as metabisulfite [$Na_2S_2O_5$] was obtained from Merck, and acetic, phosphoric acid, KCl, and sodium hydroxide from Fluka. They were purchased in the highest available purity (>99%) and were used as received.

Instruments. Stopped-Flow Spectrophotometer. Kinetic runs were carried out on a SF-300 Biokine stopped-flow multimixing spectrophotometer (dead time 3−4 ms) equipped with a millisecond visible diode-array (minimum acquisition time 0.8 ms), and a quartz microcell (path length 0.15 cm). Typical diode integration times ranged from 1 to 5 ms depending on the observed reaction. The instrument was equipped with an anaerobic gas-flushing kit, and the temperature in the mixing cell was maintained at ±0.1 °C.

pH Measurements. The pH of solutions used for kinetics measurements was determined by using a Cyberscan model 2100 pH meter and a combination electrode after calibration with standard buffer solutions. The electrode was calibrated against standard solutions of perchloric acid in THF/water 1:1 v/v 0.1 M in KCl in the acid zone, and standard solutions of KOH in THF/water 1:1 v/v 0.1 M in KCl at basic pHs.

MS-ESI Experiments. The mass spectra were recorded using a Waters Micromass ZQ series ion trap MS (ITMS) system provided with an electrospray ionization (ESI) module.

Kinetic Measurements. Stopped-Flow Measurements. HSO_3^- reacts so quickly with [Mo($S_2C_6H_4$)$_3$] and water that reaction rates were investigated using the stopped-flow technique. Depending on the reaction rate, kinetics were following scanning from 500 to 1000 spectra between 400 to 800 nm with a fast diode-array detector. Typical observation times ranged from 0.5 to 50 s. The absorbance data were corrected by subtracting a blank kinetic run in which the neutral molybdenum trisdithiolene solution was replaced by pure THF. The correction was carried out because a small absorbance change related to the mixing process was observed (see Supporting Information).

In a typical experiment, a stock solution of [Mo($S_2C_6H_4$)$_3$] (4×10^{-4} M, solution A) in dry THF, and a KOH/H_3PO_4 ($[PO_4^{3-}]_T = 0.1$ M) aqueous buffer of known pH (5.2−8.5) were prepared. Then, aqueous solutions of HSO_3^- (0.1 M, solution B), and KCl (0.1 M, solution C) were prepared using the buffer as the solvent. The reaction mixtures were prepared in situ by mixing solutions A, B, and C at 25 °C in a volumetric ratio $5{:}x{:}5-x$ (x ranging from 1 to 5) making use of the automatized mixing facilities fitted up on the SF-300 Biokine stopped-flow spectrophotometer. The injected volume of A was constant, whereas variable amounts of excess HSO_3^- (solution B) were injected. The sum of the volumes of solutions B and C, the buffer and water amounts, and the ionic strength were always the same. After mixing, the initial concentrations of reactants were 2×10^{-4} M in [Mo($S_2C_6H_4$)$_3$], 27.8 M in H_2O, and the HSO_3^- concentration ranged from 0.05 M ($x = 5$) to 0.01 M ($x = 1$). The stock solutions were prepared under anaerobic conditions. The solute was weighted in a volumetric flask which was sealed with a septum and connected to a distiller. After purging the system with the inert gas, the solvent was distilled directly into the flask under an argon current. Finally, the stock solutions were driven in the stopped-flow reservoirs by using a positive pressure of Ar. All solutions were used as soon they were prepared.

To test the influence of the buffer concentration on the kinetics, the measurements were repeated using phosphate buffers at pH = 6 whose total concentration in phosphate ranged from 0.04 to 0.12 M.

The kinetic runs were repeated at 10, 20, 30, and 40 °C ($[PO_4^{3-}]_T = 0.03$M, pH = 6) with the aim to calculate the activation parameters. Phase separation of the THF:water solutions were observed above 40 °C when buffers of $[PO_4^{3-}]_T > 0.03$ M were used.

The auto-oxidation rate of HSO_3^- was estimated by determining iodometrically the HSO_3^- concentration as a function of time. The concentration of HSO_3^- was found to decrease linearly with time during the observation period. From the slope of the line, an auto-oxidation rate of 5.7×10^{-8} mol s^{-1} L^{-1} was calculated (see Supporting Information).

MS-ESI Experiments. We have used an experimental method similar to that described by Frmeier and Metzger.[16] Stock solutions of the trisdithiolene complex in THF and aqueous solutions HSO_3^-, KOH, and NaOH were prepared. After that, the solutions were loaded into two syringes which were mounted onto a SP-200i syringe pump (from WPI) which was connected to the MS electrocapillary-line through a Teflon three valve system equipped with a mixing microchamber (from Biokine). The in-flow rate was varied from 0.05 to 0.1 mL/min (the max. in-flow rate of the MS-detector) which allowed feeding the MS electrocapillary line with a stationary-flow of fresh reaction mixture which was representative of the composition from 0.25 to 0.50 min after mixing.

The experiments were performed by direct infusion at a delivery flow of 0.05 to 0.1 mL/min using a syringe pump and a fused-silica capillary line (Polymicro Technologies) of 56 cm length (100 μm I.D. and 363 μm O.D.). The mass spectrometer conditions were 25 psi drying-nebulizer gas pressure (nitrogen) flowing at 5 L/min, T = 200 °C. The mass spectra were scanned within 70−700 m/z range, the capillary voltage was set to 3.0 kV, and 10 and 5 V were applied to skimmers 1 and 2, respectively, and 40 and 35 V for the high potential experiments. The mass spectrometer ran in negative mode at a trap-target mass of 517 m/z ([Mo($S_2C_6H_4$)$_3$] m/z). Maximum collection time was 300 ms. Typically, the mass spectra were acquired from 1 to 2 min.

Results

Rate Law. The observed stoichiometry for the reduction of [Mo($S_2C_6H_4$)$_3$] by HSO_3^- in the presence of water

(13) Cervilla, A.; Pérez-Pla, F.; Llopis, E.; Piles, M. *Inorg. Chem.* **2006**, *45*, 7357–7366.
(14) Chaudhury, P.; Nagarajan, K.; Dubey, P.; Sarkar, S. *J. Inorg. Biochemistry* **2004**, *98*, 1667–1677.
(15) Cervilla, A.; Llopis, E.; Marco, D.; Pérez-Pla, F. *Inorg. Chem.* **2001**, *40*, 6525–6528.
(16) Frmeier, S.; Metzger, J. *J. Am. Chem. Soc.* **2004**, *126*, 14485–14492.

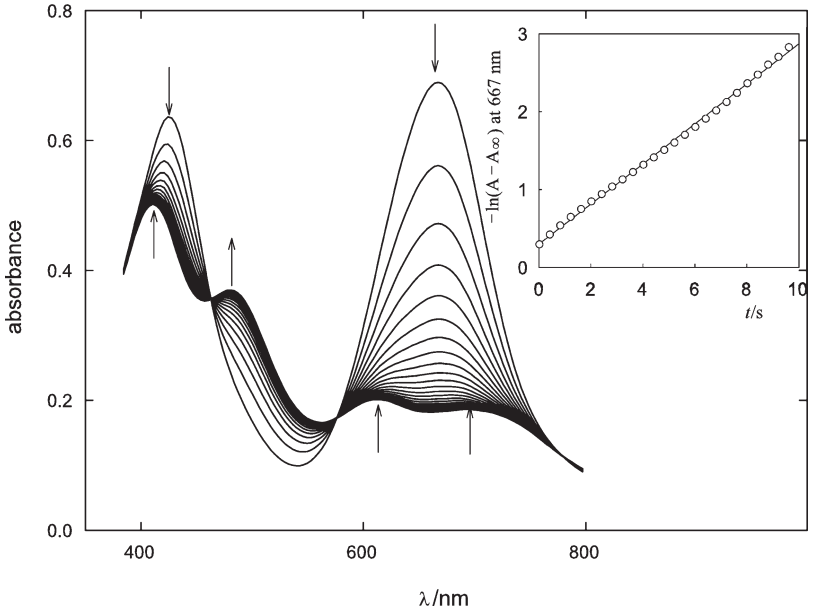

Figure 1. Visible traces monitoring the reduction of $[Mo(S_2C_6H_4)_3]$ to $[Mo(S_2C_6H_4)_3]^-$ by HSO_3^- in a phosphoric/phosphate buffer at pH = 4.14. $[[Mo(S_2C_6H_4)_3]]_0 = 3.25 \times 10^{-4}$ M; $[SO_3^{2-}]_T = 1.86 \times 10^{-2}$ M; THF/water 1:1 v/v ($[H_2O] = 27.8$ M); $T = 25$ °C. Inset: first-order plot ($-\ln(A_t - A_\infty)$ vs t) for the absorbance decay measured at 667 nm.

is given by eq 4,

$$2[Mo(S_2C_6H_4)_3] + HSO_3^- + H_2O \rightarrow 2H[Mo(S_2C_6H_4)_3] + HSO_4^- \quad (4)$$

The disappearance of sulfite was colorimetrically checked,[17] by using the Ellman test after reaction 4, and the sulfate amount formed in the resulting solutions was determined by the gravimetric analysis of $BaSO_4$. Autoxidation of sulfite in aqueous media is not uncommon but at much longer time-scales than those of the stopped-flow experiments. In fact, controls carried out in the absence of complex do not show appreciable sulfite oxidation (see Supporting Information).

Because reaction 4 was complete in a few seconds (see Supporting Information), it was monitored by stopped-flow spectrophotometry. Figure 1 illustrates the time course of a representative reaction system. The absorption bands of the neutral complex at 667 and 430 nm diminish in intensity as the reaction proceeds, and features appear at 480 and 418 nm. Three tight isosbestic points at 462, 579, and 770 nm were observed, indicating no significant accumulation of an intermediate, this point being corroborated by the analysis of the UV/vis spectra (see Supporting Information). The final spectrum is identical with that of Mo(V) measured separately which has been thoroughly characterized elsewhere.[15] Thus, Figure 1 shows the total transformation of Mo(VI) into Mo(V) within the 10 s observing time of this experiment. To determine the parameters affecting the rate of this reaction, this experiment has been performed under many varying conditions. Below, the independent effects of pH, concentration of various components, ionic strength, and temperature are discussed.

Figure 2 shows the plot of $\ln(\alpha) = \ln[(A_t - A_\infty)/(A_{t=0} - A_\infty)]$ (A, absorbance) versus time. This quantity was found to fit a straight line at any given HSO_3^- high excess concentration, demonstrating the first-order dependence of the rate law upon the $[Mo(S_2C_6H_4)_3]$ concentration. The slopes of these lines (the first-order rate constant, k_{obs}) have been plotted in Figure 3 against the total sulfite concentration ($[SO_3^{2-}]_T = [HSO_3^-] + [SO_3^{2-}]$) at several pH values. The shape of the curves is in agreement with the saturation kinetics described by eq 5,

$$-\frac{d[[Mo(S_2C_6H_4)_3]]}{dt} = \left(k_S + \frac{k_A[SO_3^{2-}]_T}{1 + k_B[SO_3^{2-}]_T}\right)[[Mo(S_2C_6H_4)_3]] \quad (5)$$

All the traces in Figure 3A show a reduced pH-dependent ordinate (k_S) originated by a slower parallel reduction of $[Mo(S_2C_6H_4)_3]$ with water (OH^-), which has been previously reported.[18,19] Experimental evidence to this effect was obtained by observing the formation of the reduced $[Mo(S_2C_6H_4)_3]^-$ complex after long-standing when $[Mo(S_2C_6H_4)_3]$ was dissolved in the phosphate buffer THF−water solution in the absence of sulfite (see line (**a**) in Figure 2). Figure 3B shows the double reciprocal plots of $(k_{obs} - k_S)$ versus $[SO_3^{2-}]_T$ ($(k_{obs} - k_S)^{-1} = 1/k_A[SO_3^{2-}]_T^{-1} + k_B/k_A$); the double reciprocal plots generate straight lines which afford k_B/k_A (the y axes intercept) and $1/k_A$ as the slope. Good straight lines were obtained in all cases confirming that $[Mo(S_2C_6H_4)_3]$ was reduced by sulfite ions following kinetics saturation.

The rate constant k_A was investigated by reducing the complex at several pH values. The relevant results of the study of the dependence of k_A upon pH are summarized in Figure 4. The k_A values drop below 10^{-2} s^{-1} M^{-1} in acidic

(17) Humphrey, R.; Ward, M.; Hinze, W. *Anal. Chem.* **1970**, *42*, 698.

(18) Cervilla, A.; Perez-Pl′a, F.; Llopis, E. *Chem. Commun.* **2001**, 2332.

(19) Cervilla, A.; Pérez-Pla, F.; Llopis, E.; Piles, M. *J. Chem. Soc., Dalton Trans.* **2004**, 1–6.

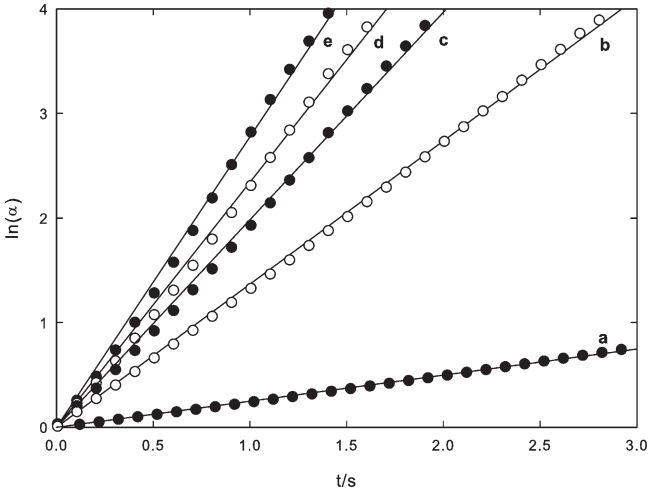

Figure 2. Plot of $\ln[(A_t - A_\infty)/(A_{t=0} - A_\infty)]$ upon time at several $[SO_3^{2-}]_T$ values. Conditions: $[SO_3^{2-}]_T \times 10^2$/M($k_{obs}$/$s^{-1}$): (**a**) 0.0 (0.27); (**b**) 1.4 (1.33); (**c**) 2.8 (1.88); (**d**) 3.5 (2.27); (**e**) 7.0 (2.51); $[Mo(S_2C_6H_4)_3]_0 = 1.8 \times 10^{-4}$ M; solvent THF/H_2O 1:1 v/v ($[H_2O]$ = 27.8 M). Phosphate buffer ($[PO_4^{3-}]_T$ = 0.1 M, pH = 8.1). T = 20.0 °C. Observation wavelength 667 nm.

media (pH ≤ 5), and increase notably in basic media (over 110 s^{-1} M^{-1} at pH > 8). The inset of figure 4 demonstrates that $\log_{10}(k_A)$ is linearly correlated to $\log_{10}(k_A + [H_3O^+])$ (representing k_A the acidic constant for hydrogen sulfite ion under the experimental conditions indicated in Figure 4), which is expressed by eq 6,

$$k_A = \frac{k}{K_A + [H_3O^+]} \quad (6)$$

In an attempt to provide information on the transition state involved in the current sulfite oxidation reaction, the dependence of k_A on ionic strength and temperature was examined. The relationship between $\log_{10}(k_A)$ and ionic strength (I) is given by the simplified Debye−Hückel equation in Figure 5A. A product charge $z_A z_B$ = 1.2 was obtained from the slope suggesting the interaction between two monoanions at the rate limiting step. The dependence of k_A on temperature at pH = 6.0 and in THF/H_2O 1:1 v/v was also examined. The k_A values were obtained from experiments similar to those plotted in Figure 3B. Figure 5B shows the Arrhenius plot for kinetic runs carried out in the temperature interval 10−40 °C. The apparent activation energy of 45 kJ mol^{-1}(≈10.8 kcal mol^{-1}) was worked out from the slope of this line.

Finally, it is remarkable that the reaction rate decreases as $[PO_4^{3-}]_T$ increases, indicating inhibition by this anion. The double reciprocal plots of k_{obs} versus $[SO_3^{2-}]_T$ at pH = 6.05 with buffers containing different overall amounts of phosphate (see Supporting Information) show the same intercept, which is typical of a competitive inhibition mechanism.[14,20] Similar experiments carried out using NaCl or Na_2SO_4 instead of sodium phosphate resulted in a non significant variation of k_A indicating that Cl^- and SO_4^{2-} anions do not act as inhibitors. Inhibition by phosphate could be explained by some kind of electrostatic binding between a phosphate and the proposed intermediate (**1**) in Scheme 1. Probably, sulfate and chloride do not inhibit the OAT due merely to their lack of basicity as electrostatic binding is expected to increase in a similar manner as the basic character of the inhibitor does.

MS-ESI Experiments. Figure 6 shows the MS-ESI spectrum recorded at a low negative ionization potential for a steady-flow obtained by continuously mixing a THF solution 1.7×10^{-4} M in $[Mo(S_2C_6H_4)_3]$ with an aqueous HSO_3^- solution 0.025 M (1:1 v/v) at room temperature. The ESI-inflow rate was maintained stationary at 0.05 mL/min during the spectra uptake, and no significant differences among spectra were found when the flow rate was increased up to 0.1 mL/min. The most relevant features of spectrum are the signals of hydrogen sulfite at m/z = 80.9, and $[Mo(S_2C_6H_4)_3]^-$ at m/z = 517, and a weak one at m/z = 394 attributable to a $[MoO(S_2C_6H_4)_2]^-$ species as assessed by the isotopic distribution analysis (see Supporting Information). The mass-spectrum indicates that the complex $[Mo(S_2C_6H_4)_3]$ is cleanly reduced to $[Mo(S_2C_6H_4)_3]^-$. The new signal was not originated as a result of fragmentation of $[Mo(S_2C_6H_4)_3]^-$ species as MS-spectra recorded at high negative ionization potential lead to the formation of $[Mo(S_2C_6H_4)_2]^-$ (m/z = 377.6), and $[HMo(S_2C_6H_4)S_2]$ (m/z = 301.6) remaining the signal at m/z = 394 unchanged.

Figure 7 shows the MS-ESI in line spectrum for a steady-flow obtained by continuously mixing a THF solution of $[Mo(S_2C_6H_4)_3]$ 1.7×10^{-4} M with aqueous solutions of KOH and NaOH 2.0×10^{-2} M (1:1 v/v). New signals at m/z = 588.70 and m/z = 604.9 appears under these conditions. The first signal is attributable to an adduct containing an unprotonated THF molecule of formula $[Mo(S_2C_6H_4)_3(C_4H_7O)]^-$, while the second one is coherent with a solvated monooxo-trisdithiolene species of formula $[MoO(S_2C_6H_4)_3(C_4H_7O)]^-$ (see Supporting Information).

Discussion

We propose that reaction 4 proceeds according to the mechanism shown in Scheme 1, which is interpreted in terms of a three-step process. The first step involves the interaction of a water molecule with $[Mo(S_2C_6H_4)_3]$, which would lead to the eventual formation of an unidentified tris-dithiolene Mo(VI)-water intermediate. Our initial proposal for the oxidation mechanism of phosphines by $[Mo(S_2C_6H_4)_3]$,[13] invoked a seven-coordinate intermediate, $[Mo(S_2C_6H_4)_3(OH)]^-$, which has been questioned based on the unique experimental results recently reported by Wieghardt et al.[21] Before this work, it was generally believed that $[Mo(S_2C_6H_4)_3]$ had the required electronic configuration (d^0) to accept a water molecule. However, its electronic structure has been recently reported as a diamagnetic ground state (S_T = 0), which is generated by intramolecular, antiferromagnetic coupling between the Mo(V) (d^1) central ion (S_M = 1/2) and a ligand π-radical dithiolene (S_{RAD} = 1/2) $Mo^V(S_2C_6H_4)_2(S_2C_6H_4)^*$.

An alternative intermediate might be a six coordinate complex (**1**), in which water coordinates to the molybdenum atom after dissociation and protonation of a thiolene group

(20) Chaudhury, P.; Das, S.; Sarkar, S. *Biochem. J.* **1996**, *319*, 953–959.

(21) Kapre, R.; Bothe, E.; Weyherm̈uler, T.; Geroge, S.; Weighardt, K. *Inorg. Chem.* **2007**, *45*, 3499–3509.

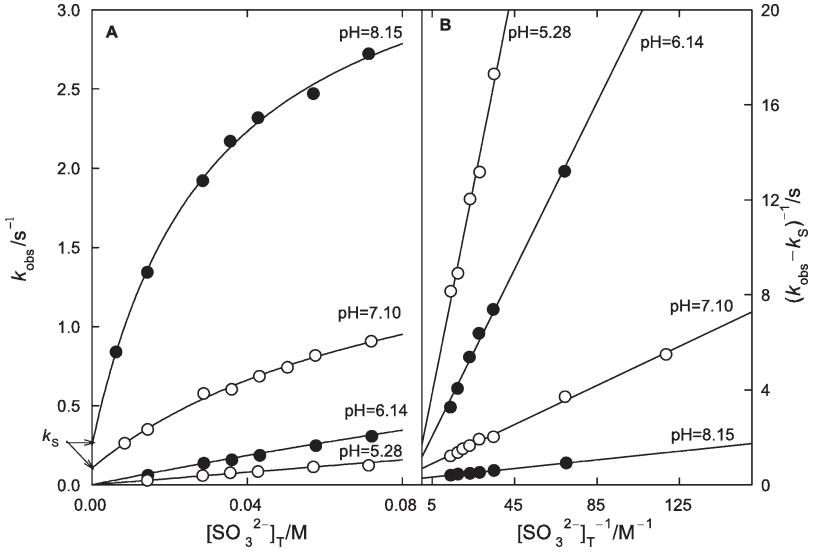

Figure 3. (A) Dependence of the first-order rate constant upon $[SO_3^{2-}]_T$ at several pH values. Conditions: $[Mo(S_2C_6H_4)_3]_0 = 2.0 \times 10^{-4}$ M; solvent THF/H_2O 1:1 v/v ($[H_2O] = 27.8$ M). Phosphate buffer ($[PO_4^{3-}]_T = 0.1$ M); $T = 20.0$ °C. Solid lines resulted from the fit of k_{obs} values to the apparent rate constant given by eq 5. (B) Double reciprocal plot of $(k_{obs} - k_S)^{-1}$ vs $[SO_3^{2-}]_T^{-1}$. The slope of these lines allows calculating the k_A rate constants.

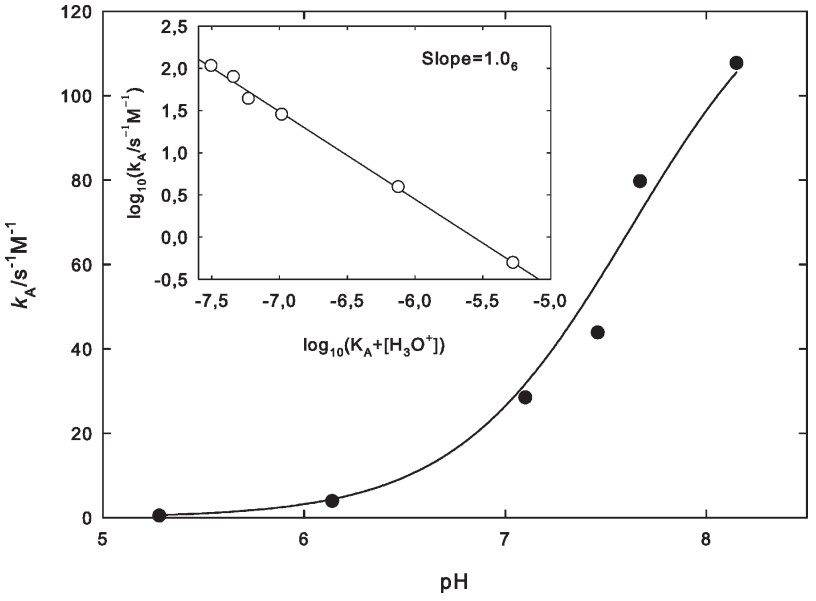

Figure 4. Variation of k_A upon pH. The solid line was calculated by fitting the k_A to eq 6 using the experimental pK_A (= 7.62) obtained from the titration curves of HSO_3^- with KOH in THF/water 1:1 v/v. Conditions: $[Mo(S_2C_6H_4)_3]_0 = 2.0 \times 10^{-4}$ M; solvent THF/H_2O 1:1 v/v ($[H_2O] = 27.8$ M). Phosphate buffer ($[PO_4^{3-}]_T = 0.1$ M); $T = 20.0$ °C. Inset: linear correlation between $\log_{10}(k_A)$ and $\log_{10}(k_A + [H_3O^+])$ expected from eq 6.

of one of the three dithiolene ligands. This step could occur in a concerted or stepwise manner, and it is therefore temptingly simple to postulate that a mono-oxo tris-dithiolene Mo(VI) may be formed. The molybdenum oxidation state controls the level of protonation of the water-based ligand and the higher oxidation state, Mo(VI), tends to have deprotonated ligands such as oxo groups.[22]

Although there is not any direct evidence of (**1**) in the mass spectrum shown in Figure 6, the rapid formation of mono-oxo-dithiolene, and monooxo-trisdithiolene species in aqueous media (see Figure 7) strongly suggest that water incorporation into the trisdithiolene complex structure is a feasible reaction. In fact, the species appearing at m/z = 604 is closely related to (**1**). A coordination environment similar to that proposed for (**1**) has been observed by Sarkar et al.[23] who have recently described the ability of $[Mo(SPh)(S_2C_2(CN)_2]^{n-}$ complexes to transfer an oxygen atom from NO_3^- to triphenylphosphine. This reaction supposedly proceeds through the intermediate $[MoO(SPh)(S_2C_2(CN)_2]^{n-}$ species, the coordination sphere of which is quite similar to that of (**1**) as they share a molybdenum center coordinated to two dithiolene ligands, one oxo-group and one sulfide.

The second step consists in the crucial hydrogen sulfite addition to the anionic intermediate (**1**) to form the adduct

(22) Stiefel, E. *Molybdenum Enzymes, Cofactors and Model Systems*; ACS Symposium serie 535; ACS: Washington, D.C, 1993.

(23) Majumdar, A.; Pal, K.; Sarkar, S. *Dalton Trans.* **2009**, *11*, 1927–1938.

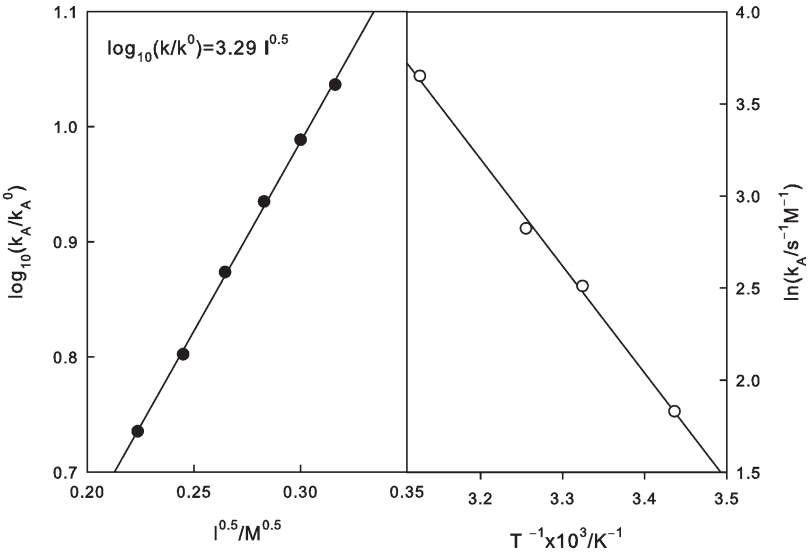

Figure 5. (A) Debye−Hückel plot for the reaction between $[Mo(S_2C_6H_4)_3]_3$ and $H_3O_3^-$. Experimental conditions: Solvent: THF/water 1:1 v/v; T = 25.0 °C; Phosphate buffer at pH = 6; The ionic strength was fixed with variable amounts of n-Bu_4NClO_4. (B) Arrhenius plot for the same reaction . Experimental conditions: Buffer: $[PO_4^{3-}]_T$ = 0.03 M at pH = 6; solvent: THF/H_2O 1:1 v/v.

Scheme 1. Reaction Mechanism[a]

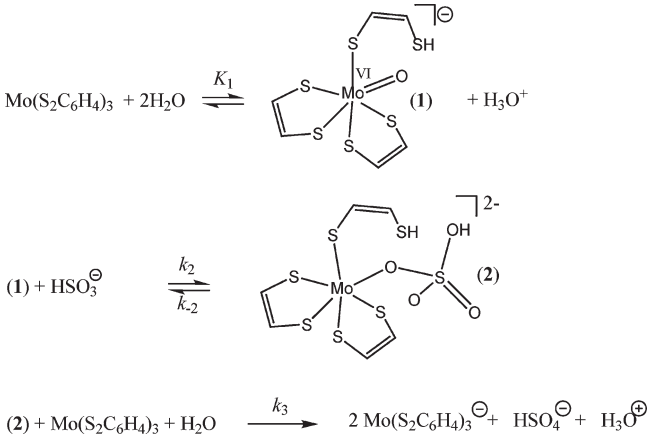

[a] The benzenic ring of $C_6H_4S_2^{2-}$ has been removed on the sake of simplicity.

(**2**). The formation of this adduct explains the dependence of k_A on the ionic strength, and allows for rationalization of the variation of the reaction rate with the dielectric constant of the medium (see Supporting Information).

Finally, we propose the last reaction depicted in Scheme 1 as the termination step, which consists of a fast electron transfer from intermediate (**2**) to excess $[Mo(S_2C_6H_4)_3]$ to yield $[Mo(S_2C_6H_4)_3]^-$ and sulfate. This is a feasible process as the Mo−O−XO_3 (X = S, P) moiety of (**2**) must exhibit a quasi-IV oxidation state.

This mechanism can be extended to phosphine oxidation[13] where a similar pH dependence on the reaction rates and saturation kinetics were observed. However, the rates of phosphine oxidation are much higher than those observed for sulfite. We attribute such rate reduction in the case of hydrogen sulfite to the charge repulsion between this anion and (**1**), which lends further support to the postulated mechanism of oxo-transfer depicted in Scheme 1.

The proposed mechanism explains the empirical rate law (eq 5) as well as the observed variation of k_A on pH, ionic strength, and temperature. The observed rate law is deduced from Scheme 1 (see Supporting Information). The expression 7 is obtained

$$\frac{1}{2}\frac{d[[Mo(S_2C_6H_4)_3]^-]}{dt} = \frac{\left(\frac{k_2K_1K_A[H_2O]^2}{K_A+[H_3O^+]}\right)[SO_3^{2-}]_T}{1+\left(\frac{(k_2/k_{-1})K_A}{K_A+[H_3O^+]}\right)[SO_3^{2-}]_T}[[Mo(S_2C_6H_4)_3]] \quad (7)$$

Equation 7 is identical to that found empirically (eq 5) after considering that

$$k_A = \frac{k_2K_1K_A[H_2O]^2}{K_A+[H_3O^+]}, \quad k_B = \frac{(k_2/k_{-1})K_A}{K_A+[H_3O^+]} \quad (8)$$

and that it is consistent that reactions conducted in excess HSO_3^- must exhibit saturation kinetics.

Equation 8 allows for discussion of the dependence of the reaction rate upon pH. The above relationship displays a $(K_A + [H_3O^+])^{-1}$ dependence of K_A which is identical to that given by the empirical eq 6. Relationship 8 appears as a result of the product of the hydrogen sulfite concentration ($[HSO_3]^- = K_A[H_3O^+]/(K_A + [H_3O^+])[SO_3^{2-}]_T$) by the factor $1/[H_3O^+]$, arising from the acid−base equilibrium involving (**1**) (see Supporting Information). This fact indicates that HSO_3^- is the active reductant in neutral or acidic media (pH of neutrality is 7.56 in THF/H_2O 1:1 v/v, pK_w = 15.13), the protonation of (**1**) causing the reaction to slow down, or even to cease, at the very acidic medium.

The interaction of hydrogen sulfite with a monocharged intermediate is corroborated by the observed variation of k_A with the ionic strength. Taking the logarithm of eq 8 affords eq 9:

$$\log_{10}(k_A) = \log_{10}\left(\frac{K_1K_A[H_2O]^2}{K_A+[H_3O^+]}\right) + \log_{10}(k_2) \quad (9)$$

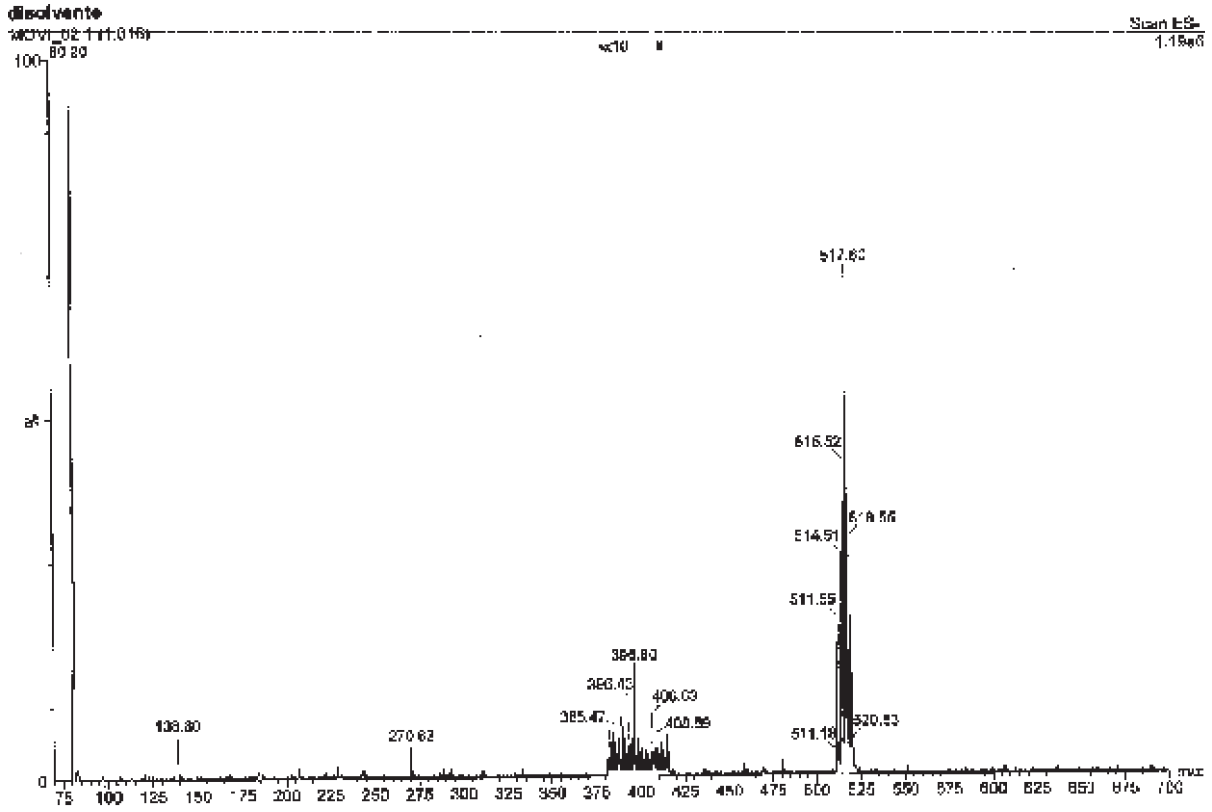

Figure 6. MS-ESI in-line spectrum of a reaction mixture 1.7×10^{-4} M in $MoO(S_2C_6H_4)_3]$ and 0.025 M inHSO_3^- ; room temperature; media: THF/water 1/1; inflow rate: 0.05 mL/min; mass-spectra taken every 1 s; accumulation time 1 min (the signal at $m/z = 394$ has been magnified $\times 10$). Spectrum recorded at low negative potential.

Equation 9 states that the variation of $\log(k_A)$ with the ionic strength (or temperature) provides direct information related to the OAT-reaction 2 in Scheme 1 between HSO_3^- and (**1**). Both terms in eq 9 are affected by ionic strength. The first one must exhibit a weak secondary saline effect owing to the fact that the quotient is dominated by the equilibrium constants K_1 and K_A. Nevertheless, the saline effect tends to cancel as these constants are appearing in the numerator and denominator of the quotient.

Interestingly, the second term must exhibit a markedly primary saline effect ruled by the Debye−Hückel equation. As shown in Figure 5A, the reaction presents a positive primary saline effect which is consistent with the reaction of two monoanionic species ($z_A z_B = 3.29/2/A = 1._2 \approx 1$, Debye−Hückel's constant $A = 1.299$ in THF/H_2O 1:1 v/v at 25 °C[24]).

This observation is in agreement with the proposal that a monoanion species, namely (**1**), is the crucial intermediate for the OAT-reaction. It is worth comparing this result with the reported saline effect of the reaction with phosphines. Thus, increasing the ionic strength has no significant effect on the phosphine oxidation rate, which is in agreement with the interaction of a neutral phosphine with the proposed monocharged intermediate. Additionally, comparison of the activation energy worked out from the Arrhenius plot in Figure 5B (11 kcal mol^{-1}) with that for the oxidation of triphenylphosphine (≈2 kcal mol^{-1}, this work, see Supporting Information) reveals that both activation energies are consistent with the formation of intermediates (**2**) and $[(S_2C_6H_4)_2(S_2C_6H_5)MoOPPh_3]^-$. The phosphine adduct requires only passing over a low activation energy barrier, which involves the interaction of the molybdenum intermediate with a neutral phosphine, whereas the formation of (**2**) requires overcoming the additional electrostatic repulsion exerted between hydrogen sulfite and (**1**) anions.

The previous results agree with an OAT-process rather than a direct electron-transfer from HSO_3^- to $[Mo(S_2C_6H_4)_3]$. Conventional sulfite chemistry[25] states that oxidation of S(IV) to S(VI) by transition metal complexes (M^{n+}) usually takes place in two steps. The first one involves the interaction of both reactants, which lends the reduced complex ($M^{(n-1)+}$) and sulfite radical,

$$M^{n+} + HSO_3^- \rightleftarrows [MSO_3H]^{(n-1)+} \rightarrow M^{(n-1)+} + \dot{S}O_3^- + H^+ \quad (10)$$

Generally, this step is followed by a fast recombination of sulfite radicals to form dithionate which, depending upon experimental conditions, disproportionates into sulfite and sulfate in aqueous media:[25,26]

$$2\dot{S}O_3^- \xrightarrow{\text{fast}} S_2O_6^{2-} \quad (11)$$

$$S_2O_6^{2-} + H_2O \rightarrow SO_4^{2-} + HSO_3^- + H^+ \quad (12)$$

(24) Roses, M.; Bosch, E. *J. Chromatograph. A* **2002**, *982*, 1–30.

(25) Neta, P.; Huie, E. *Environ. Health Perspect.* **1985**, *64*, 209–217.

(26) Liang, Y.; Gao, W.; Song, J. *Bioorg. Med. Chem. Lett.* **2006**, *16*, 5328–5333.

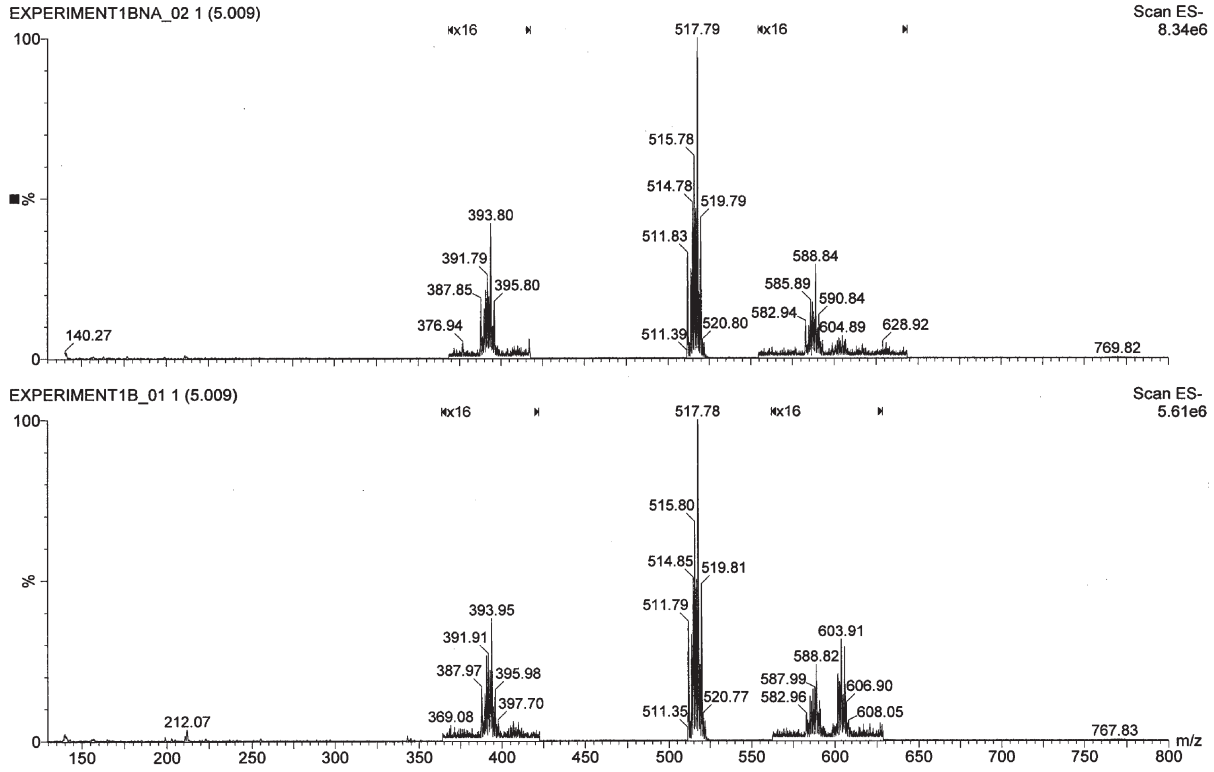

Figure 7. MS-ESI spectra obtained after mixing in-line 1:1 v/v a THF solution of $Mo(S_2C_6H_4)_3]$ 1.7×10^{-4} M with aqueous NaOH 0.02 M (upper part), and KOH 0.02 M (lower part). The signals at 394, 589, and 605 have been magnified ×16. Inflow rate: 0.05 mL/min; mass-spectra taken every 1 s; acquisition time 5 min.

or, alternatively, by a second fast electron-transfer from the sulfite radical to excess M^{n+} to form S(VI),

$$M^{n+} + \dot{S}O_3^- + 2H_2O \xrightarrow{\text{fast}} M^{(n-1)+} + HSO_4^- + H_3O^+ \quad (13)$$

The rate law deduced from this mechanism is first-order in M^{n+} and HSO_3^-, this feature being observed in most oxidations of sulfite/hydrogen sulfite anions by transition metal complexes.[25] However, $[Mo(S_2C_6H_4)_3]$ is reduced by well established monoelectronic reductants as hydrogen ascorbic acid or benzenethiol through global second-order reactions which do not present a primary saline effect (see Supporting Information).

The above observations make a difference with the kinetic behavior described in this work which clearly exhibit saturation kinetics, a fact strongly suggesting that hydrogen sulfite oxidation is following a different mechanism. This change of mechanism is probably originated by the high reduction potential of the redox pair $\dot{S}O_3^- + H^+ + e^- \rightarrow HSO_3^-$ (+840 mV NHE, water[27]) in respect to that of the pair $[Mo(S_2C_6H_4)_3] + e^- \rightarrow [Mo(S_2C_6H_4)_3]^-$, (+450 mV NHE, THF:MeOH, 20 °C), which would make the monoelectronic transfer depicted in eq 10 not spontaneous .

To date, no direct information about the coordination of the oxidized molybdenum center in sulfite oxidase is available. However, Nordlander et al.[28,30] have examined possible intermediates in the sulfite oxidase analogue reaction depicted in eq 3 by a combination of extended Hückel and density functional theory (DFT) calculations. Intermediates were considered arising from direct attack of the lone pair of HSO_3^- on the molybdenum atom to produce a seven-coordinate intermediate (see structure (**3**) in Scheme 2), or on one of the terminal oxo groups in a six-coordinate intermediate (structure (**4**)). The calculations indicate a

Scheme 2. Schematic Drawing for the Diverse Reaction Intermediates Proposed for the OAT-Reaction between $[Mo^{VI}O_2(mnt)_2]^{2-}$ and HSO_3^- [a]

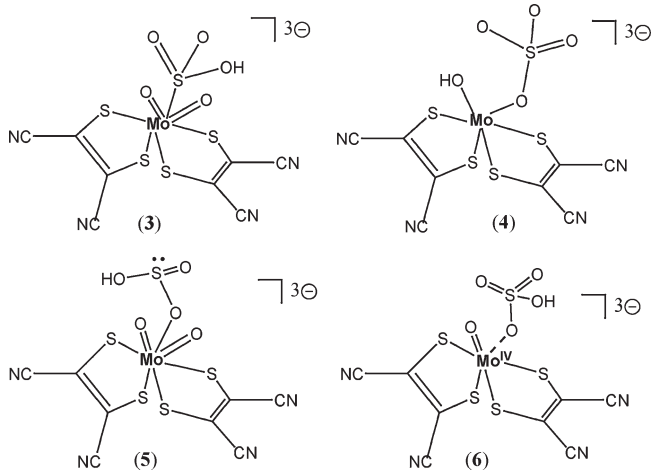

[a] (**3**) seven coordinated structure, and (**4**) six-coordinated structure calculated by Nordlander et al.;[28] (**5**) seven-coordinate, and (**6**) six-coordinate intermediates proposed by Sarkar et al.[29]

(27) Huie, E.; Neta, P. *J. Phys. Chem.* **1984**, *88*, 5665–5669.
(28) Thapper, A.; Deeth, R.; Nordlander, E. *Inorg. Chem.* **1999**, *38*, 1015–1018.
(29) Pal, K.; Chaudhury, P.; Sarkar, S. *Chem. Asian J.* **2007**, *2*, 956–964.
(30) Thapper, A.; Lorber, C.; Fryxelius, J.; Behrens, A.; Nordlander, E. *J. Inorg. Biochemistry* **2000**, *79*, 67–74.

six-coordinate intermediate formed over a barrier of about 22 kcal mol^{-1} above ground state ($[Mo^{VI}O_2(mnt)_2]^{2-}$ + HSO_3^-). The alternative pathway was higher in energy by 12 kcal mol^{-1}.

On the other hand, a recent study of Sarkar et al.[29] has analyzed the same reaction employing a similar DFT-calculation methodology. The authors have considered both the oxoanionic attack of HSO_3^- to form a seven-coordinate species containing a Mo−O−SO_3 moiety (see structure (**5**)), as well as the lone pair attack of the sulfite sulfur atom on the oxo group of the molybdenum site which eventually would form the six-coordinated intermediate proposed by Nordlander. They conclude that the oxoanionic attack proceeds through two consecutive steps. First, a seven-coordinated dioxo-complex bonded to an oxygen atom of hydrogensulfite (structure (**5**)) is formed overcoming a barrier of 22.4 kcal mol^{-1} above the ground-state. This species further evolves forming a second intermediate where the oxygen atom is transferred from molybdenum which reduces to the state (IV) (structure (**6**)). This species yield eventually the Mo(IV) and sulfate overcoming a 35.6 kcal mol^{-1} activation barrier. In contrast, calculations suggest that the lone pair attack proceeds in a single-step directly yielding the products through the Nordlander's six-coordinated intermediate which is considered in this pathway as an activated complex rather than a true reaction-intermediate. The authors conclude that the oxoanionic attack is the most probable mechanism for the OAT, since sulfite oxidation, for which both pathways are operative, present saturation kinetics, while phosphines, for which calculations indicate are reacting exclusively by the single-step lone pair attack pathway, exhibit second-order kinetics for OAT-reactions.

The results presented in this work, however, are better explained by considering the lone pair attack of sulfite on the oxo-group of (**1**) intermediate. As a difference with the Sarkar's mimetic model, OAT-reactions of $[Mo(S_2C_6H_4)_3]$ with hydrogen sulfite and phosphines exhibit both saturation kinetics, so it is reasonable to think of both reactions following similar pathways. In spite of the fact that hydrogen sulfite could coordinate (**1**) forming the Sarkar's intermediate (structure (**5**)), the main interaction between these species must occur via the formation of a Mo−O−X (X = P or S) moiety, since organic phosphines do not have oxygen atoms capable of coordinating directly to molybdenum, but present reactivity analogous to that of sulfite. On the other hand, direct attack of the lone pair of sulfite (or phosphines) on the molybdenum ion is ruled out because of the high activation barrier predicted by DFT calculations. As a consequence, the species (**2**) depicted in Scheme 1 must be considered as a true reaction intermediate and not merely a transition state. Nordlander's DFT calculations confirm the previous statement in connection with the $[Mo^{VI}O_2(mnt)_2]^{2-} + HSO_3^-$ system, while Sarkar's conclusions are just the opposite. The disagreement found among the diverse DFT calculations is not surprising since intermediate (**5**) is located inside a 0.8 kcal mol^{-1} deep potential-well, and Lee and Holm have recently demonstrated the high sensitivity of the energetics of the oxygen atom reactivity upon the calculus methodology employed.[31] As a final remark, Heinze et al.[32] have carried out an experimental and theoretical study of the OAT-reaction occurring between biomimetic molybdenum oxotransferase analogue system $[MoO_2(NN')_2]$ (*NN*′ = phenyl-(pyrrolato-2-ylmethylene)-amine) and $P(CH_3)_3$ concluding that the rate limiting step is the formation of a labile adduct formed after the phosphine lone pair attack on an oxo-group of the molybdenum complex.

As far we know, there is not experimental data available on the activation energy for the OAT from $[Mo^{VI}O_2(mnt)_2]^{2-}$ to hydrogen sulfite. This makes it difficult to compare the above-mentioned DFT energies with experimental data coming from the $[Mo^{VI}O_2(mnt)_2]^{2-} + HSO_3^-$ system, for which a barrier of 11 k cal mol^{-1} has been calculated. This relatively low activation energy reinforces the hypothesis that the OAT from a weak bonded water molecule via a Mo−O−SO_3 structure is a feasible reaction pathway. This is in agreement with recent studies performed by Enemark et al. These authors have determined the structure of the active center of *Arabidopsis thaliana*[33] and R160Q Mutant Human sulfite oxidases[34] after being reduced with sulfite in acidic media (pH ≈ 6). The reduction produces a Mo^{IV}−O−SO_3 moiety where the sulfite is bonded to the equatorial oxo-group of the active site, as the EPR spectra of the Mo^{V}−O−SO_3 containing species obtained after oxidizing with ferricyanide indicate. This result is coherent with an attack of the lone pair of sulfite on the equatorial oxo-group of the active site. As a difference with the oxo-axial, the equatorial oxo-group is labile, exhibits acid−base properties, and can be easily interchanged with water when regenerating the Mo(VI)-state of the active center during the catalytic cycle. These are, precisely, the key features of the oxo-group of the proposed intermediate (**1**). Therefore, $[Mo(S_2C_6H_4)_3]$ can also be considered as a new functional analogue of the active site of sulfite oxidase.

Concluding Remarks

In summary, the present investigation together with the previously reported phosphine oxidation system demonstrates that, regardless of the detailed mechanisms, sulfite oxidation by primary (direct) interaction with a water ligand (H_2O or OH^-) bound directly to a Mo-dithiolene moiety is a feasible reaction pathway. The evidence points to a mechanism that involves initial coordination of a water molecule to the molybdenum center, followed by proton dissociation and concerted abstraction of $2e^-$, H_3O^+ by the Mo(VI) center to give sulfate. Such mechanism is important in the context of biological processes catalyzed by some molybdoenzymes. Therefore, while we do not propose tris(dithiolene) Mo(VI) complexes as structural models for any specific molybdoenzyme, we show that their interactions with sulfite and phosphines in the presence of water incorporates the key features of the proposed oxidation mechanism of hydrogen sulfite by these catalysts. Clearly, delocalized orbitals in these complexes that involve

(31) Sonny, C.; Holm, R. *Inorg. Chim. Acta* **2008**, *361*, 1166–1176.
(32) Heinze, K.; Marano, G.; Fischer, A. *J. Inorg. Biochemistry* **2008**, *102*, 1199–1211.
(33) Astashkin, A.; Johnson-Winters, K.; Klein, E.; Byrne, R.; Hille, R.; Raitsimring, A.; Enemark, J. *J. Am. Chem. Soc.* **2007**, *129*, 14800–14810.
(34) Astashkin, A.; Johnson-Winters, K.; Klein, E.; Feng, C.; Wilson, H.; Rajagopalan, K.; Raitsimring, A.; Enemark, J. *J. Am. Chem. Soc.* **2008**, *130*, 8471–8479.

metal and multiple sulfur centers must be considered as strong candidates for the binding and activation of water, and/or the stabilization of key intermediates. According to eq 6, the value of K_A (25 s^{-1} M^{-1} at pH = 7.1), which depends on pH (Figure 4), correlates roughly with the K_2/K_M value obtained by Sarkar et al. (87 s^{-1} M^{-1}),[12] and Lorber et al. (0.26−2.5 s^{-1} M^{-1}),[35] for the $[Bu_4N]_2[Mo^{VI}O_2(mnt)_2]$ system. Thus, the order of magnitude of the rates for HSO_3^- oxidation are comparable, and, therefore, $[Mo(S_2C_6H_4)_3]$ can also be considered as a new functional analogue of the active site of sulfite oxidase.

(35) Lorber, C.; Plutino, M.; Elding, L.; Nordlander, E. J. *Chem. Soc., Dalton Trans.* **1997**, 3997.

Supporting Information Available: Additional information as noted in the text. This material is available free of charge via the Internet at http://pubs.acs.org.